

## Research Article

# Analyzing Lower Limb Dynamics in Human Gait Using Average Value-Based Technique

Sithara Mary Sunny <sup>1</sup>, K. S. Sivanandan <sup>2</sup>, Arun P. Parameswaran <sup>1</sup>,  
Baiju Thankachan <sup>3</sup> and Shyamasunder Bhat N <sup>4</sup>

<sup>1</sup>Department of Electrical and Electronics Engineering, Manipal Institute of Technology Manipal, Manipal Academy of Higher Education, Manipal, Karnataka 576104, India

<sup>2</sup>Department of Biomedical Engineering, Manipal Institute of Technology Manipal, Manipal Academy of Higher Education, Manipal, Karnataka 576104, India

<sup>3</sup>Department of Mathematics, Manipal Institute of Technology Manipal, Manipal Academy of Higher Education, Manipal, Karnataka 576104, India

<sup>4</sup>Department of Orthopaedics, Kasturba Medical College Manipal, Manipal Academy of Higher Education, Manipal, Karnataka 576104, India

Correspondence should be addressed to Arun P. Parameswaran; arun.p@manipal.edu

Received 24 August 2023; Revised 25 March 2024; Accepted 4 April 2024; Published 25 April 2024

Academic Editor: Ivan Giorgio

Copyright © 2024 Sithara Mary Sunny et al. This is an open access article distributed under the Creative Commons Attribution License, which permits unrestricted use, distribution, and reproduction in any medium, provided the original work is properly cited.

The motivation of this study is to develop effective and economical assistive technologies for people with physical disabilities. The novelty in this manuscript is the application of the average value-based technique to accurately represent the involved biomechanics of the lower limb joints during the human gait cycle. This mathematical formulation of lower limb joints' biomechanics forms the first objective for modeling and final exoskeleton prototype development. To account for modeling the characteristics of human locomotion, the  $n$ th-order linear differential equation with constant coefficients is considered with appropriate modification. The physical characteristics of an individual are represented by the constant coefficients ( $P_0$ ,  $P_1$ ,  $P_2$ , and  $P_3$ ) of the modified infinite series, which are obtained by processing experimental data collected using an optical technique. The differential terms of the infinite series are replaced by difference terms ( $\delta b_{\text{avg}}$ ,  $\delta^2 b_{\text{avg}}$ , and  $\delta^3 b_{\text{avg}}$ ) since the data were captured as a set of digital values. The work presented here is based on the experimental results of individuals suitably categorized according to their physical nature like age and other physical structure. The optically monitored positional values of the lower limb joints of the individual subjects while they are completing the gait cycles are used for getting values of different terms of the model. The data collected through the conduct of experiments are used for finding the values of the terms of the differential equation. The model is effectively validated through experimental results. It was determined that the representation's accuracy fell within the  $\pm 5\%$  acceptable tolerance limit. The model is prepared for healthy as well as disabled persons, through which the disability is quantified. The resulting model can be used to develop assistive devices for people with physical disabilities. This results in the rehabilitation process and thereby helps the reintegration into society, subsequently allowing them to lead a normal life.

## 1. Introduction

Gait analysis is a methodical examination of human locomotion that gained attention within the area of rehabilitation engineering [1–3]. The objective of rehabilitation engineering is to create advanced assistive devices that offer technological support to individuals with disabilities. The advancement of intelligent assistive devices aims to reduce the reliance of disabled individuals on others for their daily tasks, thereby

encouraging their reintegration into society [4–6]. Given the complex and nonlinear equations governing human motion, muscle dynamics, and interactions with the ground, analyzing human gait poses a challenging biomechanical problem [7, 8]. Quantifying the extent of disability in numerical terms is crucial for designing assistive devices that effectively compensate for these limitations. Direct experimentation upon a disabled person is not allowable due to ethical, psychological,

legal, and social considerations. At the same time, acquiring accurate quantified information about their condition is essential. To address this challenge, mathematical modeling of the human gait cycle comes into play.

Models offer an effective approach to investigating or evaluating the characteristics of a system, especially when direct study would be impractical without causing harm, altering the system, or interfering with its current state. In other words, modeling techniques in rehabilitation engineering offer a safe, efficient, and effective means to understand, design, and implement interventions that enhance the lives of individuals with disabilities [9, 10].

The process of analyzing models enables one to predict the potential outcomes that may arise when a system is subjected to different conditions. The field of lower limb robotics centers on conducting a thorough analytical inquiry and developing models to understand and study human gait. The primary aim of gait modeling is to develop a prediction model that can be applied to the gait patterns exhibited by individuals from different generations and characteristics. Mathematical models are developed and utilized to gain a comprehensive understanding of the underlying principles governing natural human motions. Understanding the principles of human movement is of utmost significance within the field of rehabilitation engineering.

Various modeling techniques are employed to design and optimize assistive devices, rehabilitation strategies, and technologies that aid individuals with disabilities. Some of these techniques include artificial neural networks (ANNs) [11–13], mathematical models [14], fuzzy logic [15, 16], and Petri net/S-net models. Differential equations are also extensively used to model and analyze the lower limb kinematics, muscle actions, etc., which include the inverted pendulum model of stance leg [17], muscle–tendon dynamics [18], joint torque/dynamics, and forward dynamic simulations [19].

This article discusses a novel methodology for developing and implementing mathematical models to examine the biomechanics associated with the lower limb by applying the average value technique. The formulation of a mathematical model that describes the dynamics of human mobility has the potential to yield substantial implications for the field of rehabilitation engineering [20–22]. The specific goal of the work is the simplification of the design of assistive devices for the disabled avoiding mental and physical strain. This is the prime objective of the development of this model. The suggested analytical technique makes the above-specified objective more attractive. Four cases of different disabilities are considered and quantification of disability is done through this modeling technique.

The paper is structured in the following manner: The average value-based technique is briefly introduced, followed by a description of the various steps involved in formulating the mathematical equation. The subsequent sections outline the steps involved in the determination of the constant terms, followed by the analysis of the stability of the suggested model. In the final section, the generalized mathematical equation is provided.

## 2. Average Value-Based Approach

The ordinary linear differential equation with constant coefficients is the most extensively used mathematical model for examining the dynamic response [23–27]. The idea of an average value-based model is obtained from the  $n$ th-order linear differential equations. The dynamic characteristic of a system, i.e., the input–output function of a system is represented popularly by an  $n$ th-order linear differential equation with constant coefficients between  $q_i$  the input function and  $q_o$  the output function as follows:

$$q_{\text{out}} = A_m \frac{d^m q_o}{dt^m} + A_{m-1} \frac{d^{m-1} q_o}{dt^{m-1}} + \dots + A_1 \frac{dq_o}{dt} + A_0 q_o, \quad (1)$$

$$q_{\text{input}} = B_n \frac{d^n q_i}{dt^n} + B_{n-1} \frac{d^{n-1} q_i}{dt^{n-1}} + \dots + B_1 \frac{dq_i}{dt} + B_0 q_i, \quad (2)$$

where the constants  $A$ s and  $B$ s represent the physical parameters of the system [28–30].

This equation is modified suitably to accommodate the dynamics of human locomotion. The output can be expressed as a linear combination of the base average value and an infinite number of hierarchically chosen variational terms is an assumption made here. This average value-based approach can be applied to functions having an average value. The nondifferential term is changed to a base value called base average value here, while the differential terms are changed to deviation variables [31]:

$$\begin{aligned} q_o &= \text{A base value} + \text{first variational term} \\ &+ \text{second variational term} \\ &+ \text{third variational term} + \dots \end{aligned} \quad (3)$$

The base value contains a coefficient  $A_0$  multiplied by an average value of the variable, the first variational term contains a coefficient  $A_1$  multiplied by the first variational part of the variable and the second variational term contains another coefficient  $A_2$  multiplied by the second variational part of the variable, and this process extends to infinity. While generalizing the model, these coefficients should be defined as constant values representing the physical parameters of the system, and the variable is the output of the system (in the case of an engineering system). In the case of a disabled person, physical parameters mean both—the counterpart of physical parameters of the engineering system along with psychological aspects of the subject. The extension of variational terms that must be taken into account relies on the level of accuracy that the researcher demands from the analysis.

Human locomotion is a complicated process that involves synchronous action of three subsystems (hip, knee, and ankle). The synchronous action of joints and sequential action of the legs result in linear displacement. The output, then, is the linear displacement expressed in terms of joint angular

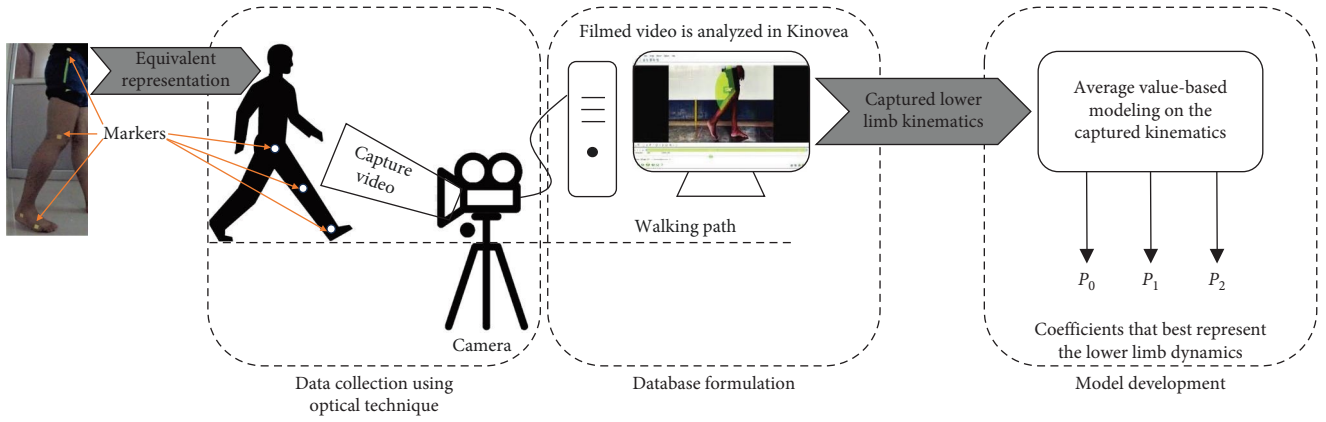


FIGURE 1: Overview of the data collection and the performed analysis.

displacement, velocity, acceleration, and jerk when the human body is regarded as the system:

$$P_0 b_{\text{avg}} + P_1 \delta b_{\text{avg}} + P_2 \delta^2 b_{\text{avg}} + P_3 \delta^3 b_{\text{avg}} = \text{Linear displacement}, \quad (4)$$

where  $P_0$ ,  $P_1$ ,  $P_2$ , and  $P_3$  are the constants that represent the physical parameters of the person and  $b_{\text{avg}}$  represents the base term,  $\delta b_{\text{avg}}$  represents the first derivative of displacement,  $\delta^2 b_{\text{avg}}$  represents the second derivative of displacement,  $\delta^3 b_{\text{avg}}$  represents the third derivative of displacement. In other words,  $b_{\text{avg}}$  represents the displacement,  $\delta b_{\text{avg}}$  represents the velocity,  $\delta^2 b_{\text{avg}}$  represents the acceleration, and  $\delta^3 b_{\text{avg}}$  represents the jerk.

The steps for developing this average value-based representation are described in the paragraphs that follow. As mentioned in the previous section, the developed mathematical model will act as a reference for the design of rehabilitative devices.

### 3. Data Collection

Gait analysis was conducted through the video analysis on 300 healthy individuals at the National Institute of Technology, Calicut, India, using a video camera having a resolution of 16.1 megapixels with 10x optical zoom, and a 25 mm wide lens which was placed perpendicular to the plane of movement. Data were collected from these 300 healthy individuals between the ages of 20 and 35 with an average weight of  $65 \pm 5$  kg and an average height of  $1.70 \pm 0.15$  m. The average thigh and shank measurements were 42 and 45 cm, respectively. This experiment includes optically monitoring and recording of [32–36] the variation in the angle at the lower limb joints and the analysis of the captured videos using Kinovea software. The camera records the positions of the joints at every 0.025 s for a total duration of 20 s. The schematic for the optical data collecting method for the positional analysis of the human leg is shown in Figure 1. Here, a single gait cycle is 1.325 s duration, of which the stance phase and swing phase, respectively, lasted 800 and 525 ms. According to an experiment performed on the participants who walked

TABLE 1: Characteristics of the subjects participated in the study.

Category	Age (years)	Weight (kgs)	Height (m)	Gait cycle duration (s)
Heathy	20–35	$65 \pm 5$	$1.7 \pm 0.15$	1.3
Patient 1	21	51	1.52	1.7
Patient 2	21	47	1.74	2.45
Patient 3	22	55	1.65	1.7
Patient 4	24	56	1.66	1.6

on a flat surface, the linear displacement was 14.4 m, the average time required to cover this displacement was 20 s, the number of gait cycles that occurred during this time was 15 on average, and the linear displacement in one gait cycle was  $\sim 0.954$  m (dataset is provided in Supplementary File).

Two female and two male patients (physically disabled individuals) were selected additionally for the study. Affected participants ranged in age from 21 to 24 years, in height from 5 to 5.7 feet, and in weight from 47 to 56 kg (Table 1). All afflicted subjects were able to walk without the aid of crutches. Subject 1 had a bent left foot but a straight right leg, Subject 2 had both legs affected by polio, Subject 3 had a longer left leg than a shorter right one, and Subject 4 had affliction in both legs (both legs bent). Except for the polio-affected person, the rest of the patients possessed the afflictions by birth.

### 4. Formulation of Mathematical Representation

This section details the algorithm for the determination of the variable terms in Equation (4). The whole dataset is divided into primary sets of equal number of elements. The nondifferential term (here referred to as the base term) is determined from the primary set. From the primary set, secondary sets are formulated, which are used to calculate the first variational term. The secondary sets are further subdivided into tertiary sets from which the second variational term is calculated. The third variational term is obtained by forming the quaternary sets from the tertiary sets [27, 37–42]. Further subsets must be generated if higher order differential terms are needed.

TABLE 2: Base mean values ( $b_{\text{avg}}$ ) of primary sets for both legs (this represents the nondifferential term of the dynamic characteristics).

Set	$b_{\text{avg}}$ of left leg Joints' dynamics			$b_{\text{avg}}$ of right leg Joints' dynamics		
	Hip	Knee	Ankle	Hip	Knee	Ankle
	Primary set A	164.615	168.235	97.985	163.13	167.855
Primary set B	163.735	165	97.461	164.22	164.93	97.75
Primary set C	163.255	164.45	97.176	164.62	165.19	97.988
Primary set D	164.47	165.03	97.899	164.585	163.855	97.967

TABLE 3: First variational terms ( $\delta b_{\text{avg}}$ ) of each set.

Set	$\delta b_{\text{avg}}$ of left leg Joints' dynamics			$\delta b_{\text{avg}}$ of right leg Joints' dynamics		
	Hip	Knee	Ankle	Hip	Knee	Ankle
	A	2.7919	5.218	1.662	3.274	6.416
B	2.512	3.92	1.495	2.058	3.956	1.225
C	2.816	6.91	1.676	2.456	7.348	1.462
D	2.336	5.034	1.39	2.558	4.626	1.523

TABLE 4: Second variational terms ( $\delta^2 b_{\text{avg}}$ ) of each set.

Set	$\delta^2 b_{\text{avg}}$ of left leg Joints' dynamics			$\delta^2 b_{\text{avg}}$ of right leg Joints' dynamics		
	Hip	Knee	Ankle	Hip	Knee	Ankle
	A	7.82	12.84	4.655	7.54	12.33
B	7.97	16.23	4.749	8.62	15.74	5.131
C	7.51	14.88	4.469	8.28	14.02	4.929
D	8.48	15.54	5.048	8.40	15.55	5.001

**4.1. Formulation of Primary Sets and Calculation of Base Term.** The initial term in the mathematical representation is the nondifferential term, also known as the base value ( $b_{\text{avg}}$ ), which is obtained by calculating the mean of the primary set. Table 2 shows the base values of each primary set. This term represents the base value, i.e., the nondifferential term of the dynamic characteristics.

**4.2. Formulation of Secondary Sets and Calculation of First Variational Term.** The primary sets are further classified into "s" subsets called secondary sets. First, the means of each secondary set are calculated. The mean of the difference between the secondary set means and the corresponding primary set's mean makes up the first variational term:

$$\delta b_{\text{avg}_A} = \text{Mean of } (A_V - A_{S1_V}), (A_V - A_{S2_V}), (A_V - A_{S3_V}), \dots, (A_V - A_{Ss_V}), \quad (5)$$

where  $A_V$  represents the primary set mean and  $A_{S1_V}, A_{S1_V}, \dots, A_{Ss_V}$ , etc., represent the mean of secondary sets. Thus, the first variational terms are calculated and are shown in Table 3.

**4.3. Formulation of Tertiary Sets and Calculation of Second Variational Term.** Tertiary sets are the next level of the division from the secondary sets after the determination of the first variational term.

Before calculating the second variational term, the means of each tertiary set are computed. The second variational term is the mean of the difference between the means of the tertiary sets and the respective secondary sets, as shown in Equation (6):

$$\delta^2 b_{\text{avg}_A} = \text{Mean of } [(A_{S1_V} - A_{T11_V}), \dots, (A_{S1_V} - A_{T1t_V}), (A_{S2_V} - A_{T21_V}), \dots, (A_{S2_V} - A_{T2t_V}), \dots, (A_{Ss_V} - A_{Ts1_V}), \dots, (A_{Ss_V} - A_{Tst_V})], \quad (6)$$

where  $s$  represents the number of secondary sets,  $t$  represents the number of tertiary sets,  $A_{S1_V}$  is the mean of the first secondary set, and  $A_{T11_V}$  is the mean of the first tertiary set of the first secondary set. The second variational term of each set is given in Table 4.

**4.4. Formulation of Quaternary Sets and Calculation of Third Variational Term.** The quaternary sets are formed which are the subdivisions of the tertiary sets. The first step in determining the third variational term is to compute the mean of each quaternary set. The third variational term is the mean of the difference between the quaternary sets' and corresponding tertiary sets' mean values:

$$\delta^3 b_{\text{avg}_A} = \text{Mean of } [(A_{T11_V} - A_{Q111_V}), \dots, (A_{T11_V} - A_{Q11q_V}), (A_{T12_V} - A_{Q121_V}), \dots, (A_{T12_V} - A_{Q12q_V}), \dots, (A_{T1t_V} - A_{Q1t1_V}), \dots, (A_{T1t_V} - A_{Q1tq_V}), \dots, (A_{Tst_V} - A_{Qst1_V}), \dots, (A_{Tst_V} - A_{Qstq_V})], \quad (7)$$

where  $t$  represents the number of tertiary sets,  $q$  represents the number of quaternary sets,  $A_{T11_V}$  is the mean of the first tertiary set, and  $A_{Q11q_V}$  is the mean of the first quaternary set of the corresponding tertiary set. The third variational term of each set is given in Table 5.

TABLE 5: Third variational terms ( $\delta^3 b_{\text{avg}}$ ) of each set.

Set	$\delta^3 b_{\text{avg}}$ of left leg			$\delta^3 b_{\text{avg}}$ of right leg		
	Joints' dynamics			Joints' dynamics		
	Hip	Knee	Ankle	Hip	Knee	Ankle
A	2.525	4.505	4.242	2.46	4.575	4.133
B	2.135	3.85	3.587	2.25	5.14	3.78
C	2.385	4.6	4.007	2.48	5.35	4.166
D	2.33	3.87	3.914	2.315	5.735	3.889

TABLE 6: The base term and the variational terms of asymmetrical gait.

Joint	$b_{\text{avg}}$	$\delta b_{\text{avg}}$	$\delta^2 b_{\text{avg}}$
Right knee	151.8	1.72	9.54
Left knee	154.6	1.88	8.58
Right hip	157.4	9.76	8.21
Left hip	153.9	6.96	12.14
Right ankle	93.69	5.81	4.886
Left ankle	90.381	1.024	5.681

Table 6 shows the different terms of the asymmetrical gait cycle. The algorithm utilized for the calculation is provided in Figure 2 for better clarity.

## 5. Average Value-Based Mathematical Representation

The modified differential equation can be written in general form as follows:

$$P_0 b_{\text{avg}} + P_1 \delta b_{\text{avg}} + P_2 \delta^2 b_{\text{avg}} + P_3 \delta^3 b_{\text{avg}} = \text{Linear displacement.} \quad (8)$$

The distance covered during the primary set's time is the linear displacement. The video is recorded for a time period of 20 s. The total distance covered in the 20 s is 14.4 m, and each primary set's covered time was 5 s. Thus, 3.6 m have been covered here.

The equations governing the gait dynamics of the left limb as shown in Equations (9)–(20). They incorporate the base value, the first variational term, the second variational term, and the third variational term.

With three variational terms:

Left knee:

$$168.235 P_0 + 5.218 P_1 + 12.84 P_2 + 4.505 P_3 = 3.6, \quad (9)$$

$$165 P_0 + 3.92 P_1 + 16.2325 P_2 + 3.85 P_3 = 3.6, \quad (10)$$

$$164.45 P_0 + 6.91 P_1 + 14.8845 P_2 + 4.6 P_3 = 3.6, \quad (11)$$

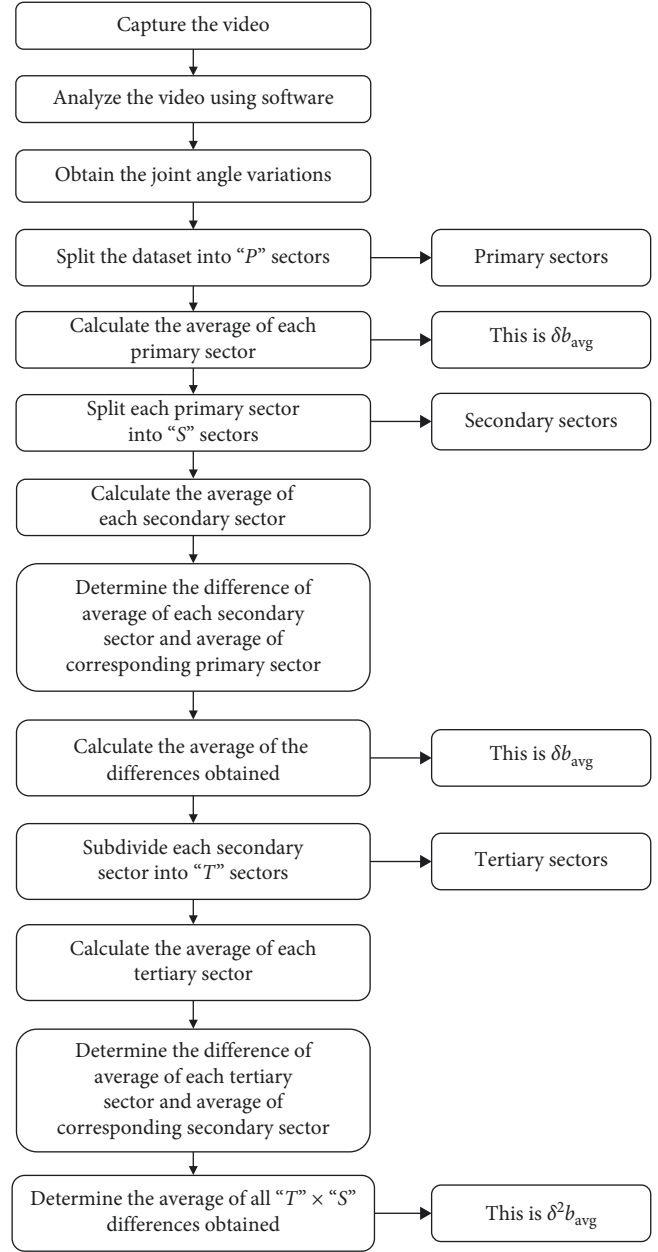


FIGURE 2: Flow diagram of average value-based method.

$$165.03 P_0 + 5.034 P_1 + 15.5425 P_2 + 3.87 P_3 = 3.6. \quad (12)$$

The equations were solved and the values for the constants  $P_0$ ,  $P_1$ ,  $P_2$ , and  $P_3$  were obtained.

Left hip:

$$164.615 P_0 + 2.7919 P_1 + 7.82 P_2 + 2.525 P_3 = 3.6, \quad (13)$$

$$163.735 P_0 + 2.512 P_1 + 7.97749 P_2 + 2.135 P_3 = 3.6, \quad (14)$$

$$163.255 P_0 + 2.816 P_1 + 7.50749 P_2 + 2.385 P_3 = 3.6, \quad (15)$$

$$164.47 P_0 + 2.336 P_1 + 8.48 P_2 + 2.325 P_3 = 3.6. \quad (16)$$

Left ankle:

$$97.985 P_0 + 1.662 P_1 + 4.655 P_2 + 1.503 P_3 = 3.6, \quad (17)$$

$$97.461 P_0 + 1.495 P_1 + 4.749 P_2 + 1.271 P_3 = 3.6, \quad (18)$$

$$97.176 P_0 + 1.676 P_1 + 4.469 P_2 + 1.42 P_3 = 3.6, \quad (19)$$

$$97.899 P_0 + 1.39 P_1 + 5.048 P_2 + 1.387 P_3 = 3.6. \quad (20)$$

The equations for the right leg are as follows:

Right knee:

$$167.855 P_0 + 6.416 P_1 + 12.33 P_2 + 4.575 P_3 = 3.6, \quad (21)$$

$$164.93 P_0 + 3.956 P_1 + 15.7425 P_2 + 5.14 P_3 = 3.6, \quad (22)$$

$$165.19 P_0 + 7.348 P_1 + 14.02 P_2 + 5.345 P_3 = 3.6, \quad (23)$$

$$163.855 P_0 + 4.626 P_1 + 15.5475 P_2 + 5.735 P_3 = 3.6. \quad (24)$$

Right hip:

$$163.13 P_0 + 3.274 P_1 + 7.54 P_2 + 2.46 P_3 = 3.6, \quad (25)$$

$$164.22 P_0 + 2.058 P_1 + 8.62 P_2 + 2.25 P_3 = 3.6, \quad (26)$$

$$164.62 P_0 + 2.456 P_1 + 8.28 P_2 + 2.478 P_3 = 3.6, \quad (27)$$

$$164.585 P_0 + 2.558 P_1 + 8.4025 P_2 + 2.315 P_3 = 3.6. \quad (28)$$

Right ankle:

$$97.101 P_0 + 1.949 P_1 + 4.488 P_2 + 1.464 P_3 = 3.6, \quad (29)$$

$$97.75 P_0 + 1.225 P_1 + 5.131 P_2 + 1.339 P_3 = 3.6, \quad (30)$$

$$97.988 P_0 + 1.462 P_1 + 4.929 P_2 + 1.476 P_3 = 3.6, \quad (31)$$

$$97.967 P_0 + 1.523 P_1 + 5.001 P_2 + 1.378 P_3 = 3.6. \quad (32)$$

With two variational terms:

Left knee:

$$168.235 P_0 + 5.218 P_1 + 12.84 P_2 = 3.6, \quad (33)$$

$$165 P_0 + 3.92 P_1 + 16.2325 P_2 = 3.6, \quad (34)$$

$$164.45 P_0 + 6.91 P_1 + 14.8845 P_2 = 3.6, \quad (35)$$

$$165.03 P_0 + 5.034 P_1 + 15.5425 P_2 = 3.6. \quad (36)$$

The equations were solved and the values for the constants  $P_0$ ,  $P_1$ , and  $P_2$  were obtained.

Left hip:

$$164.615 P_0 + 2.7919 P_1 + 7.82 P_2 = 3.6, \quad (37)$$

$$163.735 P_0 + 2.512 P_1 + 7.97749 P_2 = 3.6, \quad (38)$$

$$163.255 P_0 + 2.816 P_1 + 7.50749 P_2 = 3.6, \quad (39)$$

$$164.47 P_0 + 2.336 P_1 + 8.48 P_2 = 3.6. \quad (40)$$

Left ankle:

$$97.985 P_0 + 1.662 P_1 + 4.655 P_2 = 3.6, \quad (41)$$

$$97.461 P_0 + 1.495 P_1 + 4.749 P_2 = 3.6, \quad (42)$$

$$97.176 P_0 + 1.676 P_1 + 4.469 P_2 = 3.6, \quad (43)$$

$$97.899 P_0 + 1.39 P_1 + 5.048 P_2 = 3.6. \quad (44)$$

The equations for the right leg are as follows:

Right knee:

$$167.855 P_0 + 6.416 P_1 + 12.33 P_2 = 3.6, \quad (45)$$

$$164.93 P_0 + 3.956 P_1 + 15.7425 P_2 = 3.6, \quad (46)$$

TABLE 7: Obtained values of constants with three variational terms.

Limb details	$P_0$	$P_1$	$P_2$	$P_3$
Left leg				
Hip	0.04031	-0.4537	-0.2671	0.1269
Knee	0.01915	0.01418	0.02371	0.00016
Ankle	0.0672	-0.7476	-0.4414	0.20755
Right leg				
Hip	0.03103	-0.05906	-0.1241	-0.1352
Knee	0.01943	0.00264	0.01256	0.03625
Ankle	0.0521	-0.0993	-0.20826	-0.22588

$$165.19 P_0 + 7.348 P_1 + 14.02 P_2 = 3.6, \quad (47)$$

$$163.855 P_0 + 4.626 P_1 + 15.5475 P_2 = 3.6. \quad (48)$$

Right hip:

$$163.13 P_0 + 3.274 P_1 + 7.54 P_2 = 3.6, \quad (49)$$

$$164.22 P_0 + 2.058 P_1 + 8.62 P_2 = 3.6, \quad (50)$$

$$164.62 P_0 + 2.456 P_1 + 8.28 P_2 = 3.6, \quad (51)$$

$$164.585 P_0 + 2.558 P_1 + 8.4025 P_2 = 3.6. \quad (52)$$

Right ankle:

$$97.101 P_0 + 1.949 P_1 + 4.488 P_2 = 3.6, \quad (53)$$

$$97.75 P_0 + 1.225 P_1 + 5.131 P_2 = 3.6, \quad (54)$$

$$97.988 P_0 + 1.462 P_1 + 4.929 P_2 = 3.6, \quad (55)$$

$$97.967 P_0 + 1.523 P_1 + 5.001 P_2 = 3.6. \quad (56)$$

## 6. Results and Discussion

The values for the constants  $P_0$ ,  $P_1$ ,  $P_2$ , and  $P_3$  are determined by solving Equations (9)–(32) (i.e., considering up to third variational term). For the left knee, the values for  $P_0$ ,  $P_1$ ,  $P_2$ , and  $P_3$  were 0.01915, 0.01418, 0.02371, and 0.00016, respectively. For the right knee, the values were 0.01943, 0.00264, 0.01256, and 0.03625. For the hip, the values were determined to be 0.04031, -0.4537, -0.2671, and 0.1269 for the left hip, and 0.03103, -0.05906, -0.1241, and -0.1352 for the right hip. When the ankle joint is considered, 0.0672, -0.7476, -0.4414, and 0.20755 for the left ankle and 0.0521, -0.0993, -0.2082, and -0.22588 for the right ankle. The values obtained are shown in Table 7.

The values for the constants  $P_0$ ,  $P_1$ , and  $P_2$  are determined by solving Equations (33)–(56) (i.e., considering up to the second variational term). For the left knee, the values for  $P_0$ ,  $P_1$ , and  $P_2$  were 0.01914, 0.01422, and 0.02374, respectively. For the right knee, the values were 0.0168, 0.02553, and 0.04666. For the hip, the values were determined to be

TABLE 8: Obtained values of constants with two variational terms.

Limb details	$P_0$	$P_1$	$P_2$
Left leg			
Hip	0.03006	-0.1557	-0.1163
Knee	0.01914	0.01422	0.02374
Ankle	0.05056	-0.26157	-0.1953
Right leg			
Hip	0.01575	0.09302	0.09465
Knee	0.0168	0.02552	0.04666
Ankle	0.02646	0.15627	0.15901

0.03006, -0.1557, and -0.1163 for the left hip and 0.01575, 0.09302, and 0.09465 for the right hip. For the left ankle, the values for  $P_0$ ,  $P_1$ , and  $P_2$  were 0.05056, -0.26157, and -0.1953, respectively. For the right ankle, the values were 0.02646, 0.15627, and 0.15901. The values obtained are shown in Table 8. The equations for validation are as follows:

$$163.51 P_0 + 5.296 P_1 + 15.2225 P_2 + 4.59 P_3, \quad (57)$$

$$166.715 P_0 + 8.608 P_1 + 12.81 P_2 + 5.205 P_3, \quad (58)$$

$$163.415 P_0 + 2.818 P_1 + 7.665 P_2 + 2.255 P_3, \quad (59)$$

$$164.47 P_0 + 2.336 P_1 + 8.48 P_2 + 2.33 P_3, \quad (60)$$

$$97.271 P_0 + 1.677 P_1 + 4.562 P_2 + 1.342 P_3, \quad (61)$$

$$97.899 P_0 + 1.39 P_1 + 5.048 P_2 + 1.387 P_3. \quad (62)$$

Equation (57) is the equation of left knee joint, Equation (58) is the equation of right knee joint, Equation (59) is the equation of left hip joint, Equation (60) is the equation of right hip joint, Equation (61) is the equation of left ankle joint, and Equation (62) is the equation of right ankle joint. The values of  $P_0$ ,  $P_1$ , and  $P_2$  shown in Tables 7 and 8 are substituted and the error is calculated and shown in Table 9. It could be seen from Table 9 that there is not much difference in errors with and without considering the third variational term. Hence for the easiness of calculation, till the second variational term can be considered.

The gait cycle is completed in 1.3 s for healthy subjects and 1.6–2.45 s for afflicted ones. Because of practical and statutory constraints, only four patients could be examined. This study reveals that each affliction has its unique characteristics and a general affliction characteristic specification seems difficult. The experimental observations produced a quantified way for declaring the disability of the abovementioned cases. The disability is defined in terms of the displacement magnitude ratio between hip/knee, hip/ankle, and knee/ankle. These ratios are obtained by comparing the same with the counterpart of the healthy subject (this value is taken on an average basis upon the results of 300 subjects). The ratio of the displacement magnitude of hip/knee, hip/ankle, and knee/ankle are shown in Table 10. Table 11

TABLE 9: Comparison of the error of the model formulated with two variational terms and three variational terms.

Joint	Error	
	Up to the second variational term	Up to the third variational term
Left knee	0.032961	0.032861
Right knee	0.01738	0.0135
Left hip	0.01725	0.00538
Right hip	0.010363	0.0021046
Left ankle	-0.0115	0.000819
Right ankle	0.0103	0.000853

TABLE 10: Various joint angle displacement magnitude ratios (hip to knee (H/K), hip to ankle (H/A), knee to ankle (K/A)) of healthy and afflicted patients.

Subject	Right leg			Left leg		
	H/K ratio	H/A ratio	K/A ratio	H/K ratio	H/A ratio	K/A ratio
Healthy	1.0093	1.68	1.699	1.0068	1.68	1.7026
Patient 1	1.0281	1.9518	1.9058	0.9718	1.951	2.0418
Patient 2	0.987	1.771	1.8051	1.0255	1.646	1.608
Patient 3	0.9499	1.549	1.634	0.9607	1.6039	1.675
Patient 4	0.965	1.998	2.061	0.9954	1.999	2.009

TABLE 11: Difference in ratios of hip to knee (H/K), hip to ankle (H/A), and knee to ankle (K/A) of both legs of afflicted patients.

Subject	Right leg			Left leg		
	H/K ratio	H/A ratio	K/A ratio	H/K ratio	H/A ratio	K/A ratio
Afflicted 1	-0.01875	-0.27162	-0.20586	0.034968	-0.27029	-0.33912
Afflicted 2	0.02764	-0.09077	-0.10515	-0.01915	0.033497	0.094203
Afflicted 3	0.059371	0.130485	0.065893	0.046043	0.076051	0.027721
Afflicted 4	0.044246	-0.31484	-0.36813	0.011297	-0.31962	-0.30725

TABLE 12: Calculated percentage of the affliction of afflicted subjects in hip/knee (H/K) ratio, hip/ankle (H/A) ratio, and knee/ankle (K/A) ratio of both legs of each subject.

Subject	Right leg			Left leg		
	H/K ratio	H/A ratio	K/A ratio	H/K ratio	H/A ratio	K/A ratio
Afflicted 1	-1.856	-16.17	-12.11	3.474	-16.08	-19.92
Afflicted 2	2.74	-5.403	-6.186	-1.9021	1.99	5.533
Afflicted 3	5.889	7.767	3.876	4.575	4.527	1.628
Afflicted 4	4.385	-18.74	-21.654	1.122	-19.02	-18.045

shows the difference in the ratio of healthy and afflicted subjects. The percentage of affliction is calculated using the ratio values as follows:

$$\text{Percentage of affliction} = \frac{(\text{Ratio of healthy subjects} - \text{Ratio of disabled subject})}{\text{Ratio of healthy subjects}} \quad (63)$$

The percentage of affliction corresponding to each afflicted subject is shown in Table 12.

Equation (8) represents the dynamic properties of human locomotion. Therefore, the researchers may confidently assert that, on average, the dynamic characteristics of a healthy individual are accessible for various physical attributes such as height, weight, and so on. The dynamic characteristics of the impaired person can also be obtained. By determining physical attributes such as weight, height, etc., it becomes possible to compare them with those of a healthy individual. Through this comparison, clinical specialists can potentially measure the extent of disability in the individual with disabilities. This greatly aids the rehabilitation engineer in designing appropriate assistive equipment. This demonstrates the practical significance of the model.



TABLE 13: Validation of the joints' dynamics (right leg).

Joint	$b_{avg}$	$\delta b_{avg}$	$\delta^2 b_{avg}$	Output	Error	Mean of the error
Right knee	166.845	5.914	12.74	3.54755	0.05245	0.02103
	166.515	4.622	15.548	3.64006	-0.04006	
	162.985	4.986	14.88	3.5589	0.0411	
	165.485	8.958	11.05	3.52354	0.07646	
	167.765	4.342	12.13	3.49443	0.10557	
	166.715	8.608	12.81	3.61739	-0.01739	
	162.88	5.326	15.732	3.60556	-0.00556	
	164.47	8.254	14.242	3.63746	-0.03746	
	169.745	3.746	12.025	3.50757	0.09243	
	165.465	6.788	14.195	3.61457	-0.01457	
Right hip	164.61	6.662	15.243	3.64589	-0.04589	0.00534
	162.01	8.602	13.165	3.55477	0.04523	
	163.51	2.752	7.855	3.57478	-0.02522	
	164.59	2.732	8.085	3.6117	0.0117	
	164.62	2.686	7.842	3.5849	-0.0151	
	163.835	3.152	7.677	3.60026	0.00026	
	163.255	2.816	7.507	3.54378	-0.05622	
	164.47	2.336	8.48	3.61036	0.01036	
	164.62	2.286	8.5	3.60997	0.00997	
	164.21	2.738	7.977	3.59605	-0.00395	
Right ankle	164.62	2.456	8.28	3.60496	0.00496	-0.0070725
	164.22	2.058	8.62	3.59382	-0.00618	
	163.13	3.274	7.54	3.58754	-0.01246	
	164.585	2.178	8.695	3.61783	0.01783	
	97.327	1.638	4.676	3.6252	-0.0252	
	97.97	1.626	4.812	3.5885	0.0115	
	97.988	1.599	4.668	3.6151	-0.0151	
	97.521	1.876	4.57	3.5998	0.0002	
	97.176	1.676	4.469	3.6562	-0.0562	
	97.899	1.39	5.048	3.61031	-0.01031	
97.988	1.36	5.06	3.59	0.01		
97.744	1.63	4.749	3.6038	-0.0038		
97.988	1.462	4.929	3.59501	0.00499		
97.75	1.225	5.131	3.60622	-0.00622		
97.101	1.949	4.488	3.6125	-0.0125		
97.967	1.296	5.176	3.58223	0.01777		

6.1. *Stability Analysis.* The stability of the model is assessed by replicating the analysis using a distinct dataset comprising individuals from the same age group who exhibit comparable physical traits and health conditions. Since it is clear from the comparison table (Table 9) that the difference in error that is produced by taking into account up to two variational terms as opposed to taking into account up to three variational terms is insignificant, the validation is performed by just taking into account up to two variational terms. The output obtained and the error are given in Tables 13 and 14.

### 7. Generalization of Mathematical Equation

Once the constants have been determined, the linear differential equation can be expressed in matrix form, with  $k$  being

the constant term added which needs to be determined for each individual and  $D$  representing the linear displacement.

Rewriting Equation (4) results in the following equations:

$$(P_0 \ P_1 \ P_2 \ P_3) \begin{pmatrix} X \\ \delta b_{avg} \\ \delta^2 b_{avg} \\ \delta^3 b_{avg} \end{pmatrix} + k = D, \tag{64}$$

$$X = \frac{1}{N_m} \sum_{i_m=1}^{N_m} X_{i_m}, \tag{65}$$

where  $N_m$  is the total number of elements of primary set,  $X_{i_m}$  is the element in the set, and  $X$  is the  $b_{avg}$ .

TABLE 14: Validation of the joints' dynamics (left leg).

Joint	$b_{\text{avg}}$	$\delta b_{\text{avg}}$	$\delta^2 b_{\text{avg}}$	Output	Error	Mean of the error
Left knee	166.785	4.658	14.493	3.60334	-0.00334	0.01049
	162.705	5.786	15.988	3.57676	0.02324	
	166.89	4.852	14.143	3.59981	0.00019	
	166.335	6.902	13.192	3.59575	0.00425	
	168.81	7.212	11.157	3.59923	0.00077	
	163.51	5.296	15.222	3.56703	0.03297	
	166.3	5.41	14.142	3.59642	0.00358	
	164.095	4.634	16.337	3.59528	0.00472	
	165.245	3.076	14.835	3.5595	0.0405	
	167.735	7.192	12.05	3.59957	0.00043	
	162.385	5.642	15.968	3.56812	0.03188	
	167.35	8.48	12.17	3.61335	-0.01335	
Left hip	164.405	2.132	8.665	3.60302	0.00302	0.01073
	163.195	3.016	7.453	3.56996	-0.03004	
	163.855	2.336	8.137	3.61613	0.01613	
	164.62	2.928	7.73	3.59428	-0.00572	
	164.56	2.638	8.182	3.58507	-0.01493	
	163.415	2.818	7.665	3.58274	-0.01726	
	163.51	2.752	7.855	3.57378	-0.02622	
	164.59	2.852	7.775	3.59998	-2E-05	
	163.62	2.654	7.882	3.5892	-0.0108	
	164.605	2.784	8.04	3.5802	-0.0198	
	164.62	2.756	7.675	3.62746	0.02746	
	163.23	2.836	7.88	3.54937	-0.05063	
Left ankle	97.86	1.269	5.518	3.5915	0.0085	-0.005815
	97.14	1.795	4.436	3.6245	-0.0245	
	97.533	1.39	4.844	3.5783	0.0217	
	97.988	1.743	4.601	3.6002	-0.0002	
	97.952	1.57	4.871	3.6095	-0.0095	
	97.271	1.677	4.562	3.6116	-0.0116	
	97.327	1.638	4.676	3.628	-0.028	
	97.97	1.698	4.628	3.5946	0.0054	
	97.393	1.58	4.692	3.60544	-0.00544	
	97.979	1.657	4.786	3.61431	-0.01431	
	97.988	1.64	4.568	3.5668	0.0332	
	97.161	1.688	4.69	3.64503	-0.04503	

$$A_i = \frac{1}{N_{s_i}} \sum_{s_i=1}^{N_{s_i}} X_{s_i}, \quad (66)$$

$$B_{ij} = \frac{1}{N_{t_j}} \sum_{j=1}^{N_{t_j}} X_{t_j}, \quad (68)$$

where  $N_{s_i}$  is the number of elements in the  $i$ th secondary set and  $A_i$  is its mean.

where  $B_{ij}$  is the mean of the tertiary set and  $N_{t_j}$  is the number of elements in the tertiary set considered corresponding to the  $i$ th secondary set.

$$\delta b_{\text{avg}} = \frac{1}{w} \sum_{i=1}^w (X - A_i), \quad (67)$$

$$\delta^2 b_{\text{avg}} = \frac{1}{w} \sum_{i=1}^w \frac{1}{m} \sum_{j=1}^m (A_i - B_{ij}), \quad (69)$$

where  $w$  is the number of secondary sets.

where  $m$  is the number of tertiary sets and  $w$  is the number of secondary sets.

Secondary sets are further divided into subsets known as tertiary sets. Suppose each secondary set is subdivided into  $m$  tertiary sets:

Tertiary sets are further divided into subsets known as quaternary sets. Suppose each tertiary set is subdivided into  $p$  quaternary sets:

$$C_{ijp} = \frac{1}{N_{q_p}} \sum_{p=1}^{N_{q_p}} X_{q_p}, \quad (70)$$

where  $C_{ijp}$  is the mean of the quaternary set and  $N_{q_{ijp}}$  is the number of elements in the quaternary set considered corresponding to the  $i$ th secondary set and  $j$ th tertiary set.

$$\delta^3 b_{\text{avg}} = \frac{1}{w} \sum_{i=1}^w \frac{1}{m} \sum_{j=1}^m \frac{1}{q} \sum_{p=1}^q (B_{ij} - C_{ijp}), \quad (71)$$

where  $q$  is the number of quaternary sets,  $m$  is the number of tertiary sets, and  $w$  is the number of secondary sets. Here,  $k$  is taken as zero as the psychological parameters are not considered.

## 8. Conclusion

The purpose of this research was to develop a mathematical model of lower limb joint dynamics that might be applied to the development of assistive devices for people with physical disabilities. The variation of lower limb joint angles for different subjects of different heights, weights, and ages was recorded, analyzed, and tabulated considering time as the independent variable. The novelty in this manuscript is the application of the average value-based technique to accurately represent the biomechanics of the lower limb joints during the human gait cycle. Real-time analysis of various gait cycles (without making any assumptions) obtained from the walking profiles of various subjects ensures the robustness and practicality of the adopted modeling process.

The average value-based mathematical representation is a modified version of the  $n$ th ordinary linear differential equation. The  $n$ th ordinary linear differential equation can be used to express a system's dynamic properties as an input-output function with constant coefficients [24, 43]. This has been modified to take into account the dynamics of the disabled individual. An infinite series' nondifferential term is denoted by the average of the primary set,  $b_{\text{avg}}$ . The primary set is further split up into secondary sets to calculate the first variational term ( $\delta b_{\text{avg}}$ ). The subset split can be performed as many times as the required number of variational terms. The degree of accuracy that the researcher seeks determines how many variational terms must be taken into account. In this study, the representation with three variational terms and two variational terms was developed. The error was calculated considering the second variational term and the third variational term. It was observed that the difference in error was very low. Hence, for ease of calculation, dynamics can be represented by considering up to the second variational term.

Constant terms ( $P_0, P_1, P_2, \dots$ , etc.) are used to reflect the subject's physical characteristics. A set of equations is developed to determine the value of constant terms. The equations were developed and solved using Python software and thereby the constant term values were determined. The obtained constant values are substituted in Equation (4). The developed mathematical model will serve as a foundation for developing rehabilitation-related assistive technology. Biomechanics and motor control methods utilized during functional motions

can be better understood with the help of models. They provide insights into mechanisms of afflicted movement due to disability. Using models, rehabilitation interventions such as orthoses, prostheses, robotic devices, and therapy activities can be fine-tuned for each patient. Models facilitate accurate performance predictions for emerging rehabilitative technology and aid in establishing design parameters that align with user capabilities.

The limitations of the current study include the fact that the developed model is not applicable to all age groups and that the study focuses only on physical aspects and overlooks psychological parameters. However, both psychological and physical factors have an impact on dynamics. It is not included in the current model-building process in order to reduce the complexity involved. The addition of a constant term, as discussed in the previous section, may, however, make up for this flaw. The objective of this study was limited to an accurate mathematical representation of the lower limb dynamics during a human gait cycle. The results of this modeling procedure will be used in future studies to develop the prototype of an intelligent human lower limb exoskeleton.

## Data Availability

The data used to support the findings of this study are available from the corresponding author upon request.

## Conflicts of Interest

The authors declare that they have no conflicts of interest.

## Acknowledgments

The authors acknowledge the financial assistance offered by Manipal Academy of Higher Education (MAHE)—(MAHE/CDS/PHD/IMF/2019). Open access funding enabled and organized by MANIPAL 2023. The authors acknowledge the computational facility offered by the Manipal Institute of Technology in Manipal, India, as well as the technical help obtained from the National Institute of Technology in Calicut.

## Supplementary Materials

The supplementary file contains data of the angles at the three lower limb joints (hip, knee, and ankle) of the healthy as well as afflicted subjects. 300 healthy subjects took part in the experiment. The participants were directed to walk on a flat surface, with a linear displacement of 14.4 m, the average time required to cover this displacement was 20 s. Variations of lower limb joint angles of four afflicted subjects were also collected. All the afflicted subjects were able to walk without the aid of crutches. The captured videos were analyzed using Kinovea software. (*Supplementary Materials*)

## References

- [1] V. Bijalwan, V. B. Semwal, and T. K. Mandal, "Fusion of multi-sensor-based biomechanical gait analysis using vision and wearable sensor," *IEEE Sensors Journal*, vol. 21, no. 13, pp. 14213–14220, 2021.

- [2] V. B. Semwal, R. Jain, P. Maheshwari, and S. Khatwani, "Gait reference trajectory generation at different walking speeds using LSTM and CNN," *Multimedia Tools and Applications*, vol. 82, pp. 33401–33419, 2023.
- [3] A. Gupta and V. B. Semwal, "Occluded Gait reconstruction in multi person Gait environment using different numerical methods," *Multimedia Tools and Applications*, vol. 81, pp. 23421–23448, 2022.
- [4] A. Guatibonza, L. Solaque, and A. Velasco, "Parallel assistive robotic system for knee rehabilitation: kinematic and dynamic modeling validation," *Journal of Medical Engineering & Technology*, vol. 46, no. 8, pp. 637–647, 2022.
- [5] R. Rathor, A. K. Singh, H. Choudhary, C. Goswami, and G. Fekete, "A systematic review on gait analysis methods and assistive devices in lower limb prosthetics," *Materials Today: Proceedings*, vol. 44, Part 6, pp. 4251–4255, 2021.
- [6] L. Shelmerdine and G. Stansby, "Lower limb amputation and rehabilitation," *Surgery*, vol. 40, no. 7, pp. 445–449, 2022.
- [7] M. Ezati, B. Ghannadi, and J. McPhee, "A review of simulation methods for human movement dynamics with emphasis on gait," *Multibody System Dynamics*, vol. 47, pp. 265–292, 2019.
- [8] K. Yamane and Y. Nakamura, "Robot kinematics and dynamics for modeling the human body," in *Robotics Research: The 13th International Symposium ISRR*, pp. 49–60, Springer, Berlin, Heidelberg, 2010.
- [9] A. F. Guatibonza, L. Solaque, and A. Velasco, "Kinematic and dynamic modeling of a 5-bar assistive device for knee rehabilitation," in *2018 IEEE Third Ecuador Technical Chapters Meeting (ETCM)*, pp. 1–6, IEEE, Cuenca, Ecuador, October 2018.
- [10] S. M. Sunny, K. S. Sivanandan, A. P. Parameswaran, T. Baiju, and N. Shyamasunder Bhat, "Application of artificial neural network for successful prediction of lower limb dynamics and improvement in the mathematical representation of knee dynamics in human locomotion," in *International Conference on Robotics, Control, Automation and Artificial Intelligence*, pp. 921–932, Springer Nature, Singapore, 2022.
- [11] M. Raj, V. B. Semwal, and G. C. Nandi, "Bidirectional association of joint angle trajectories for humanoid locomotion: the restricted Boltzmann machine approach," *Neural Computing and Applications*, vol. 30, pp. 1747–1755, 2018.
- [12] V. B. Semwal, A. Mazumdar, A. Jha, N. Gaud, and V. Bijalwan, "Speed, cloth and pose invariant gait recognition-based person identification," in *Machine Learning: Theoretical Foundations and Practical Applications*, pp. 39–56, Springer, Singapore, 2021.
- [13] V. Semwal, G. Singh, U. Crespo, and R. González, "Heterogeneous computing model for post-injury walking pattern restoration and postural stability rehabilitation exercise recognition," *Expert Systems*, vol. 39, no. 6, Article ID e12706, 2021.
- [14] S. Glowinski, T. Krzyzynski, A. Bryndal, and I. Maciejewski, "A kinematic model of a humanoid lower limb exoskeleton with hydraulic actuators," *Sensors*, vol. 20, no. 21, Article ID 6116, 2020.
- [15] R. Sharma, P. Gaur, S. Bhatt, and D. Joshi, "Optimal fuzzy logic-based control strategy for lower limb rehabilitation exoskeleton," *Applied Soft Computing*, vol. 105, Article ID 107226, 2021.
- [16] T. S. Sangeetha, S. M. Sunny, K. S. Sivanandan, A. P. Parameswaran, and T. Baiju, "Development of a software-based driving system module for lower limb exoskeleton," *AIP Conference Proceedings*, vol. 2875, no. 1, Article ID 020007, 2023.
- [17] A. D. Kuo, J. M. Donelan, and A. Ruina, "Energetic consequences of walking like an inverted pendulum: step-to-step transitions," *Exercise and Sport Sciences Reviews*, vol. 33, no. 2, pp. 88–97, 2005.
- [18] I. E. Brown and G. E. Loeb, "A reductionist approach to creating and using neuromusculoskeletal models," in *Biomechanics and Neural Control of Posture and Movement*, pp. 148–163, Springer, New York, NY, 2000.
- [19] J. M. Wakeling, M. Febrer-Nafria, and F. De Groote, "A review of the efforts to develop muscle and musculoskeletal models for biomechanics in the last 50 years," *Journal of Biomechanics*, vol. 155, Article ID 111657, 2023.
- [20] R. Sun, S. Sharaf, and B. J. Ali, "Human gait modelling and tracking based on motion functionalisation," *Applied Mathematics and Nonlinear Sciences*, vol. 7, no. 2, pp. 21–30, 2021.
- [21] V. E. Berbyuk and B. A. Lytvyn, "Mathematical modeling of human walking on the basis of optimization of controlled processes in biodynamical systems," *Journal of Mathematical Sciences*, vol. 104, pp. 1575–1586, 2001.
- [22] V. B. Semwal, P. Tokas, M. Nilesh, and N. Khare, "Dynamic balancing of bipedal robot on inclined terrain using polynomial trajectories," in *ICGSP '23: Proceedings of the 2023 7th International Conference on Graphics and Signal Processing*, pp. 72–77, Association for Computing Machinery, Fujisawa, Japan, June 2023.
- [23] V. B. Semwal, Y. Kim, V. Bijalwan et al., "Development of the LSTM model and universal polynomial equation for all the sub-phases of human gait," *IEEE Sensors Journal*, vol. 23, no. 14, pp. 15892–15900, 2023.
- [24] E. O. Doebelin and D. N. Manik, *Measurement Systems: Application and Design*, McGraw-Hill, 2007.
- [25] J. Schmalz, D. Paul, K. Shorter, X. Schmalz, M. Cooper, and A. Murphy, *Modelling Human Gait using a Nonlinear Differential Equation*, Cold Spring Harbor Laboratory, 2021.
- [26] S. Glowinski and T. Krzyzynski, "An inverse kinematic algorithm for the human leg," *Journal of Theoretical and Applied Mechanics*, vol. 54, no. 1, pp. 53–61, 2016.
- [27] T. S. Jobin Varghese, K. S. Sivanandan, and P. K. Rajendrakumar, "Modelling analysis and realization of a supporting system for afflicted subjects," *International Journal of Scientific & Engineering Research*, vol. 5, no. 5, pp. 1–7, 2014.
- [28] S. Banerjee, *Mathematical Modeling: Models, Analysis and Applications*, Chapman and Hall/CRC, 2021.
- [29] E. Doebelin, *System Dynamics: Modeling, Analysis, Simulation, Design*, CRC Press, 1998.
- [30] S. M. Sunny, K. S. Sivanandan, B. Thankachan, and A. P. Parameswaran, "Mathematical modeling and analysis of biological systems," *Global and Stochastic Analysis*, vol. 11, pp. 51–63, 2024.
- [31] T. S. Sirish, K. S. Sivanandan, J. Varghese, and P. K. Rajendrakumar, "Modelling, analysis and fabrication of supporting system for lower limb," *International Journal of Scientific Engineering & Technology*, vol. 3, no. 4, pp. 428–432, 2014.
- [32] J. J. L. Wang and S. Singh, "Video analysis of human dynamics—a survey," *Real-Time Imaging*, vol. 9, no. 5, pp. 321–346, 2003.
- [33] S. Glowinski, A. Blazejewski, and T. Krzyzynski, "Inertial sensors and wavelets analysis as a tool for pathological gait identification," in *Innovations in Biomedical Engineering*, pp. 106–114, Springer, Cham, 2017.
- [34] B. Kwolek, A. Michalczuk, T. Krzeszowski, A. Switonski, H. Josinski, and K. Wojciechowski, "Calibrated and synchronized multi-view video and motion capture dataset for evaluation of gait recognition," *Multimedia Tools and Applications*, vol. 78, pp. 32437–32465, 2019.
- [35] S. K. Challa, A. Kumar, V. B. Semwal, and N. Dua, "An optimized-LSTM and RGB-D sensor-based human gait

- trajectory generator for bipedal robot walking,” *IEEE Sensors Journal*, vol. 22, no. 24, pp. 24352–24363, 2022.
- [36] V. B. Semwal, N. Gaud, P. Lalwani, V. Bijalwan, and A. K. Alok, “Pattern identification of different human joints for different human walking styles using inertial measurement unit (IMU) sensor,” *Artificial Intelligence Review*, vol. 55, pp. 1149–1169, 2022.
- [37] T. S. Sirish, “*Modeling, analysis and realization of supporting system for afflicted human locomotion*,” Ph.D. thesis, National Institute of Technology Calicut, 2014.
- [38] S. M. Sunny, K. S. Sivanandan, A. P. Parameswaran, T. Baiju, and N. Shyamasunder Bhat, “A novel technique to mathematically represent the human knee dynamics through the application of the integral concept,” in *2022 International Conference on Distributed Computing, VLSI, Electrical Circuits and Robotics (DISCOVER)*, pp. 180–185, IEEE, Shivamogga, India, October 2022.
- [39] M. Ashmi, “*Development and implementation of an assistive drive mechanism for afflicted human beings*,” Ph.D. thesis, National Institute of Technology Calicut, 2018.
- [40] V. Sujalakshmy, K. S. Sivanandan, and K. M. Moideenkutty, “Average value based model for electrical distribution system load dynamics,” *International Journal of Electrical Power & Energy Systems*, vol. 43, no. 1, pp. 1285–1295, 2012.
- [41] T. S. Sirish, V. Sujalakshmy, and K. S. Sivanandan, “A new approach for modeling the system dynamics,” *Global Journal of Researches in Engineering: F Electrical and Electronics Engineering*, vol. 12, no. 1, pp. 37–47, 2012.
- [42] O. I. Abiodun, A. Jantan, A. E. Omolara, K. V. Dada, N. A. E. Mohamed, and H. Arshad, “State-of-the-art in artificial neural network applications: a survey,” *Heliyon*, vol. 4, no. 11, Article ID e00938, 2018.
- [43] C. D. Johnson, *Process Control Instrumentation Technology*, Pearson, 2014.